
p -Laplacian Transformer

Tuan Nguyen
Toyo University
Tokyo, Japan

Tam Nguyen
Rice University
Houston, USA

Vinh Nguyen
FPT AI Center
Vietnam

Tan M. Nguyen
National University of Singapore
Singapore

Abstract

p -Laplacian regularization, rooted in graph and image signal processing, introduces a parameter p to control the regularization effect on these data. Smaller values of p promote sparsity and interpretability, while larger values encourage smoother solutions. In this paper, we first show that the self-attention mechanism obtains the minimal Laplacian regularization ($p = 2$) and encourages the smoothness in the architecture. However, the smoothness is not suitable for the heterophilic structure of self-attention in transformers where attention weights between tokens that are in close proximity and non-close ones are assigned indistinguishably. From that insight, we then propose a novel class of transformers, namely the p -Laplacian Transformer (p-LaT), which leverages p -Laplacian regularization framework to harness the heterophilic features within self-attention layers. In particular, low p values will effectively assign higher attention weights to tokens that are in close proximity to the current token being processed. We empirically demonstrate the advantages of p-LaT over the baseline transformers on a wide range of benchmark datasets.

1 Introduction

In recent years, Transformer models have risen to prominence in the field of machine learning, achieving remarkable success in various domains, including natural language processing (Brown et al., 2020; Dai et al., 2019; Raffel et al., 2020), reinforcement learning (Chen et al., 2021), computer vision (Dosovitskiy

et al., 2020; Liu et al., 2021; Arnab et al., 2021; Guo et al., 2021), and various practical applications (Rives et al., 2021; Jumper et al., 2021; Gulati et al., 2020; Zhang et al., 2019). What distinguishes Transformers is their proficiency in transferring knowledge from pre-trained models to new tasks, even when data is limited (Radford et al., 2018, 2019; Devlin et al., 2018; Liu et al., 2019).

At the core of Transformers lies the self-attention mechanism, a fundamental component that calculates weighted averages of token representations within a sequence. These weightings are determined by assessing similarity scores between pairs of tokens, thereby establishing their relative significance in the sequence. This intrinsic adaptability in capturing a wide array of syntactic and semantic relationships has been identified as a pivotal factor contributing to the triumph of Transformers (Vaswani et al., 2017; Vig and Belinkov, 2019; Voita et al., 2019).

1.1 Self-attention Mechanism

Given an input sequence denoted as $\mathbf{X} := [\mathbf{x}(1), \dots, \mathbf{x}(N)]^\top \in \mathbb{R}^{N \times D_x}$, self-attention operates by initially projecting \mathbf{X} into three distinct matrices: the query matrix $\mathbf{Q} := [\mathbf{q}(1), \dots, \mathbf{q}(N)]^\top$, the key matrix $\mathbf{K} := [\mathbf{k}(1), \dots, \mathbf{k}(N)]^\top$, and the value matrix $\mathbf{V} := [\mathbf{v}(1), \dots, \mathbf{v}(N)]^\top$. These transformations are achieved through linear operations as described by the following equations:

$$\mathbf{Q} = \mathbf{X}\mathbf{W}_Q^\top; \mathbf{K} = \mathbf{X}\mathbf{W}_K^\top; \mathbf{V} = \mathbf{X}\mathbf{W}_V^\top \quad (1)$$

Here, \mathbf{W}_Q and $\mathbf{W}_K \in \mathbb{R}^{D_q \times D_x}$, while $\mathbf{W}_V \in \mathbb{R}^{D_v \times D_x}$.

Each query vector $\mathbf{q}(i)$ corresponds to a specific token at the i -th position, and the attention scores from this token to all other tokens are computed by taking the dot product $\mathbf{q}(i)^\top \mathbf{k}$ between the query vector $\mathbf{q}(i)$ and the key vectors $\mathbf{v}(j)$. Subsequently, the output vector $\mathbf{u}(i)$ is determined by a weighted sum according to the formula:

$$\mathbf{u}(i) = \sum_{j=1}^N \text{softmax} \left(\mathbf{q}(i)^\top \mathbf{k}(j) / \sqrt{D_{qk}} \right) \mathbf{v}(j) \quad (2)$$

Alternatively, the output sequence $\mathbf{U} := [\mathbf{u}(1), \dots, \mathbf{u}(N)]^\top \in \mathbb{R}^{N \times D_{qk}}$ can be computed as:

$$\mathbf{U} = \text{softmax} \left(\mathbf{Q}\mathbf{K}^\top / \sqrt{D_{qk}} \right) \mathbf{V} := \mathbf{A}\mathbf{V}$$

Here, the softmax function is applied row-wise. The matrix \mathbf{A} , denoted as the softmax attention matrix, belongs to $\mathbb{R}^{N \times N}$ and its elements represent the computed attention scores.

1.2 Multi-Head Self-Attention

The Multi-Head Self-Attention (MSA) mechanism plays a pivotal role in the Transformer architecture, a core component that empowers these models with their remarkable capabilities. MSA leverages a group of self-attention heads, seamlessly combining their outputs through a linear projection (Vaswani et al., 2017)

$$\text{MSA}(\mathbf{X}) := \text{FFN}([\mathbf{U}^1, \dots, \mathbf{U}^H])$$

Here, H represents the total number of attention heads, and \mathbf{U}^h represents the output of the self-attention mechanism at the h -th head. Each head is equipped with its parameter sets $\mathbf{W}_Q^h; \mathbf{W}_K^h; \mathbf{W}_V^h$, corresponding to the query, key, and value matrices $\{\mathbf{Q}^h; \mathbf{K}^h; \mathbf{V}^h\}$ as defined in Equation (1).

The final linear projection, denoted as FFN, can be expressed as:

$$\text{FFN}(\mathbf{X}) := \mathbf{X}\mathbf{W}_O$$

Here, $\mathbf{W}_O \in \mathbb{R}^{HD_{qk} \times D_{qk}}$ serves as the essential operator that projects the multi-head outputs into the corresponding hidden dimensions. Besides MSA module, each transformer block is equipped with a skip connections to cooperate with MSA. Formally, a transformer layer l -th can be written as follows:

$$\mathbf{U}_{(l+1)} = \text{MSA}(\mathbf{U}_l) + \mathbf{U}_l$$

1.3 Transformers and Heterophily structures

Heterophily, which is often associated with a disassortative structure, characterizes networks where connected nodes tend to belong to different classes or exhibit dissimilar attributes. It’s a concept deeply rooted in network science, reflecting the propensity of diverse elements to connect. Heterophily can manifest in a variety of domains, for instance, in a network based on

word adjacencies in text, where the labels represent the part of speech (POS) of each word, it’s common to observe that adjacent words frequently have distinct POS labels (Gu et al., 2023). Words, even when closely positioned within the text, often serve different linguistic functions, leading to this inherent diversity in their attributes. Another notable example can be found in the realm of protein chemistry, where chemical interactions often occur between different types of amino acids (Li et al., 2022). However, it’s important to note that the current self-attention, primarily designed for tasks involving homophilic structures, is not suitable for effectively modeling heterophily relationships.

In general, Self Attention operates by updating token representations through the aggregation of information from other tokens, effectively acting as a kind of low-pass filter (Wang et al., 2022). This filter primarily emphasizes the commonalities in token features while inadvertently downplaying their differences, resulting in a homogenization of learned token representations. The inherent smoothness of low-frequency information makes this mechanism well-suited for networks exhibiting homophily where connected nodes tend to belong to the same classes or similar attributes. However, for heterophilic networks, applying a smoothing filter across connections may not be ideal, as it encourages connected nodes to resemble each other predictably, contradicting the nature of disassortativity. For instance, imposing similar representations on connected proteins through a low-pass filter would significantly impede performance, as the low-frequency information struggles to support inferences within such networks. In such cases, high-frequency information, which captures the nuanced differences between nodes, may offer a more appropriate solution.

1.4 Contribution

Under heterophily, it is crucial to leverage both similarities and dissimilarity between the node features in a neighborhood to be able to learn high-quality representations. However, without having access to the labels, it is not clear how the node features in a neighborhood should be aggregated. To address the above challenge, our key idea is to leverage a low-pass filter in a typical Transformers encoder to capture both similarities and dissimilarities of nodes with their neighborhood and generate representations.

One potential approach to address this issue is through the nonlocal framework. In nonlocal framework (Gilboa and Osher, 2009), image patches are treated as nodes in a weighted graph, with each edge assigned a value that quantifies the similarity between the corresponding nodes. We can formally formulate the relationships between patches and their collective role

within the entire image. This enables a more thorough study of the intricacies of images. Additionally, this approach allows for a convenient definition of energy functionals and can be further put into PDE-like evolutions for comprehensive processing and analysis (Rudin et al., 1992). Furthermore, it has been shown that self-attention is closely related to the nonlocal framework (Wang et al., 2018; Ramachandran et al., 2019). In this study, we delve into the p -Laplacian regularization framework as a fundamental component of our exploration, to understand its implications for the self-attention mechanism and performance of Transformers.

Our main contributions can be summarized as follows

1. We use p -Laplacian Regularization Framework to show that the self-attention mechanism obtains the minimal p -laplacian regularized functional in the case of $p = 2$.
2. Motivated from p -Laplacian Regularization Framework, we propose p -Laplacian Transformers (p -LaT).
3. We theoretically prove that p -LaT guarantees the convergence of p -LaT and can alleviate the low-pass filter effect.

We empirically demonstrate the advantages of p -LaT on various large-scale applications, including the ImageNet object classification, and WikiText-103 language modeling tasks.

Organization. Our paper follows this structured path: In Section 2, we reveal the intrinsic link between self-attention and the p -Laplacian regularization framework, particularly when $p = 2$. Section 3 introduces the novel p -LaT model, underpinned by theoretical guarantees of convergence. A comprehensive spectral analysis in Section 4 showcases the non-low-pass filters characteristic in p -LaT. Section 5 is dedicated to empirical validation across various benchmarks. We provide context within the realm of related work in Section 6, and in our concluding section, we summarize our contributions and offer broader insights.

2 Self-attention is a particular case of p -regularization

In this section, we establish a strong connection between traditional self-attention mechanisms and the p -Laplacian regularization framework. Specifically, we derive Equation (2) from the p -Laplacian regularization framework, in the case where $p = 2$. We then reveal that a layer of self-attention can be viewed as a step in the minimization process of a functional. This

connection not only enhances our understanding of self-attention but also underscores the adaptability of the p -Laplacian regularization framework beyond its conventional domain in image processing.

We first consider the output matrix $\mathbf{U} := [\mathbf{u}(1), \dots, \mathbf{u}(N)]^\top \in \mathbb{R}^{N \times D}$ in (2) be a real vector-valued function, i.e., $\mathbf{u} : \Omega \rightarrow \mathbb{R}^D$, $u \in C^2(\Omega)$ with $\Omega \in \mathbb{R}$ and $x \in \Omega$. Then we can present the process of minimizing the following p -laplacian regularized functional

$$J(\mathbf{u}) = \frac{1}{p} \int_{\Omega^2} k(x, y) \|\mathbf{u}(y) - \mathbf{u}(x)\|^p dydx \quad (3)$$

To minimize the functional $J(\mathbf{u})$, we proceed by assuming that there is $\mathbf{u} \in C^2(\bar{\Omega})$ so that $J(\mathbf{u}) \leq J(\mathbf{v})$ for all $\mathbf{v} \in C^2(\bar{\Omega})$ and $\mathbf{u} = \mathbf{v}$ on $\partial\Omega$. Now, let $h \in C_c^\infty(\Omega)$ and set $\mathbf{v} = \mathbf{u} + t\mathbf{h}$ for a real number t . Thus, by the above assumption we have

$$J(\mathbf{u}) \leq J(\mathbf{v}) = J(\mathbf{u} + t\mathbf{h}) \quad \forall t \in \mathbb{R}$$

This indicates that $J(\mathbf{u} + t\mathbf{h})$ has a global minimum at $t = 0$. Now we need to solve the following equation to minimize (3)

$$\left. \frac{d}{dt} \right|_{t=0} J(\mathbf{u} + t\mathbf{h}) = 0 \quad (4)$$

For simplicity, we define $I : \mathbb{R}^D \rightarrow \mathbb{R}$, $I(Q) = Q^p$.

This yields

$$\begin{aligned} \left. \frac{d}{dt} J(\mathbf{u} + t\mathbf{h}) \right|_{t=0} &= \frac{1}{p} \int_{\Omega^2} k(x, y) \left. \frac{d}{dt} I(\mathbf{u}(x) - \mathbf{u}(y)) \right|_{t=0} \\ &\quad + t(\mathbf{h}(x) - \mathbf{h}(y)) dx dy \\ \left. \frac{d}{dt} J(\mathbf{u} + t\mathbf{h}) \right|_{t=0} &= \frac{1}{p} \int_{\Omega^2} k(x, y) \nabla I(\mathbf{u}(x) - \mathbf{u}(y)) \\ &\quad + t(\mathbf{h}(x) - \mathbf{h}(y)) (\mathbf{h}(x) - \mathbf{h}(y)) dx dy \end{aligned}$$

Therefore, from (4) we have

$$\begin{aligned} \left. \frac{d}{dt} \right|_{t=0} J(\mathbf{u} + t\mathbf{h}) &= \frac{1}{p} \int_{\Omega^2} k(x, y) \nabla I(\mathbf{u}(x) - \mathbf{u}(y)) \\ &\quad (\mathbf{h}(x) - \mathbf{h}(y)) dx dy = 0 \end{aligned}$$

Or,

$$\begin{aligned} \frac{1}{p} \int_{\Omega^2} k(x, y) \nabla I(\mathbf{u}(x) - \mathbf{u}(y)) \mathbf{h}(x) dx dy \\ - \frac{1}{p} \int_{\Omega^2} k(x, y) \nabla I(\mathbf{u}(x) - \mathbf{u}(y)) \mathbf{h}(y) dx dy = 0 \end{aligned}$$

and change of variable $(x, y) \rightarrow (y, x)$ in the second integral and with

$$\nabla I(\mathbf{u}(x) - \mathbf{u}(y)) = p \|\mathbf{u}(x) - \mathbf{u}(y)\|^{p-2} (\mathbf{u}(x) - \mathbf{u}(y))$$

we obtain

$$\int_{\Omega^2} K(x, y) \|\mathbf{u}(x) - \mathbf{u}(y)\|^{p-2} (\mathbf{u}(x) - \mathbf{u}(y)) \mathbf{h}(x) dx dy = 0 \quad (5)$$

where $K(x, y) := k(x, y) + k(y, x)$ is a symmetric kernel.

Since (5) is true for all $h \in C^\infty(\Omega)$, we deduce

$$\int_{\Omega} K(x, y) \|\mathbf{u}(x) - \mathbf{u}(y)\|^{p-2} (\mathbf{u}(x) - \mathbf{u}(y)) dy = 0 \quad (6)$$

To numerically compute solutions of (6), one could use the gradient descent method, which corresponds to solving the PDE

$$\begin{aligned} \frac{d\mathbf{u}(x, t)}{dt} &= - \int_{\Omega} K(x, y) \mathbf{p}(x, y) (\mathbf{u}(x) - \mathbf{u}(y)) dy \\ \mathbf{p}(x, y) &= \|\mathbf{u}(x) - \mathbf{u}(y)\|^{p-2} \end{aligned} \quad (7)$$

We discretize the ODE in (7) using Euler method with step size $\Delta t = 1 / \int_{\Omega} K(x, y) dy$ and obtaining the following

$$\begin{aligned} \mathbf{u}(x, \Delta t) &= \mathbf{u}(x, 0) + \\ \Delta t \int_{\Omega} K(x, y) \|\mathbf{u}(x, 0) - \mathbf{u}(y, 0)\|^{p-2} (\mathbf{u}(y, 0) - \mathbf{u}(x, 0)) dy & \\ &= \int_{\Omega} \frac{K(x, y) \|\mathbf{u}(x, 0) - \mathbf{u}(y, 0)\|^{p-2}}{\int_{\Omega} K(x, y') dy'} \mathbf{u}(y, 0) dy \\ &= \int_{\Omega} \frac{K(x, y)}{\int_{\Omega} K(x, y') dy'} \mathbf{u}(y, 0) dy \end{aligned}$$

the last line is obtained by setting $p = 2$.

Let $\mathbf{v}(x) := [v_1(x), \dots, v_D(x)]^\top$ be a real vector-valued function, where $\mathbf{v} : \Omega \rightarrow \mathbb{R}^D$, $\mathbf{v} \in C^2(\Omega)$. We set initial value of \mathbf{u} with $\mathbf{v}(x)$, i.e., $\mathbf{u}(x, 0) = \mathbf{v}(x)$. Similar to $\mathbf{v}(x)$, we define $\mathbf{k}(x) := [k_1(x), \dots, k_{D_{qk}}(x)]^\top$ be a real vector-valued function, where $\mathbf{k} : \Omega \rightarrow \mathbb{R}^{D_{qk}}$, $\mathbf{k} \in C^2(\Omega)$. We choose $K(x, y) = \exp(\mathbf{k}(x)^\top \mathbf{k}(y) / \sqrt{D_{qk}})$ and using Monte-Carlo approximation, we could rewrite the above equation as following

$$\begin{aligned} \mathbf{u}(x, \Delta t) &\approx \sum_{y=1}^N \frac{\exp(\mathbf{k}(x)^\top \mathbf{k}(y) / \sqrt{D_{qk}})}{\sum_{y'=1}^N \exp(\mathbf{k}(x)^\top \mathbf{k}(y') / \sqrt{D_{qk}})} \mathbf{v}(y) \\ &\approx \sum_{y=1}^N \text{softmax} \left(\mathbf{k}(x)^\top \mathbf{k}(y) / \sqrt{D_{qk}} \right) \mathbf{v}(y) \end{aligned} \quad (8)$$

Comparing (8) and (2), we observe that (8) implement a symmetric self-attention, in which the query matrix \mathbf{Q} and the key matrix \mathbf{K} are identical, i.e. $\mathbf{W}_Q = \mathbf{W}_K$ where \mathbf{W}_Q and \mathbf{W}_K are the linear projections that map the input sequence \mathbf{X} into \mathbf{Q} and \mathbf{K} as given in (1). If we relax this symmetry condition, in other words, we replace the key vectors $\mathbf{k}(x)$ with the query vectors $\mathbf{q}(x)$, $x = 1, \dots, N$, to obtain the exact formula of self-attention given by (2) would be obtained. The following theorem summarizes our above result

Theorem 2.1. *Given the p -laplacian regularized functional $J(\mathbf{u}) = \frac{1}{p} \int_{\Omega^2} k(x, y) \|\mathbf{u}(y) - \mathbf{u}(x)\|^p dy dx$ of a vector-valued function $\mathbf{u} : \Omega \rightarrow \mathbb{R}^D$, $\mathbf{u} \in C^2(\Omega)$. The corresponding gradient flow to minimize $J(\mathbf{u})$ is $\frac{d\mathbf{u}(x, t)}{dt} = - \int_{\Omega} K(x, y) \|\mathbf{u}(x) - \mathbf{u}(y)\|^{p-2} (\mathbf{u}(x) - \mathbf{u}(y)) dy$ where $K(x, y) = \exp(\mathbf{k}(x)^\top \mathbf{k}(y) / \sqrt{D_{qk}})$ and $\mathbf{k} : \Omega \rightarrow \mathbb{R}^D$, $\mathbf{k} \in C^2(\Omega)$. Then, taking an Euler discretization method with initial value $\mathbf{u}(x, 0) = \mathbf{v}(x)$ and step size $\Delta t = 1 / \int_{\Omega} K(x, y) dy$ is equivalent to a symmetric self-attention*

$$\mathbf{u}(x) = \sum_{y=1}^N \text{softmax} \left(\mathbf{k}(x)^\top \mathbf{k}(y) / \sqrt{D_{qk}} \right) \mathbf{v}(y) \quad (9)$$

Breaking the symmetry of the attention scores by replacing $\mathbf{k}(x)$ with $\mathbf{q}(x)$, $x = 1, \dots, N$, in (9), we obtain the exact formula of self-attention

$$\mathbf{u}(x) = \sum_{y=1}^N \text{softmax} \left(\mathbf{q}(x)^\top \mathbf{k}(y) / \sqrt{D_{qk}} \right) \mathbf{v}(y) \quad (10)$$

3 p -Laplacian Transformers

In this section, we derive the p -Laplacian-based self-attention equation from a p -Laplacian regularization framework and present p -LaT, a new Transformers architecture developed upon the new self-attention scheme. We then provide a theoretical result that the new self-attention scheme is guaranteed to converge.

Following the derivations from section 2, from ODE (7), we again discretize using the Euler method, but this time, with arbitrary p value and step size $\Delta t = 1 / \int_{\Omega} K(x, y) dy$, initial value $\mathbf{u}(x, 0) = \mathbf{v}(x)$

$$\mathbf{u}(x, \Delta t) = \int_{\Omega} \frac{K(x, y)}{\int_{\Omega} K(x, y') dy'} \|\mathbf{v}(x) - \mathbf{v}(y)\|^{p-2} \mathbf{v}(y) dy$$

Then choose $K(x, y) = \exp(\mathbf{k}(x)^\top \mathbf{k}(y) / \sqrt{D_{qk}})$ and using the Monte-Carlo method, we would obtain the following new formula for calculating symmetric self-attention

$\mathbf{u}(x, \Delta t) \approx$

$$\sum_{y=1}^N \text{softmax} \left(\frac{\mathbf{k}(x)^\top \mathbf{k}(y)}{\sqrt{D_{qk}}} \right) \|\mathbf{v}(x) - \mathbf{v}(y)\|^{p-2} \mathbf{v}(y)$$

By replacing the key vectors $\mathbf{k}(x)$ with the query vectors $\mathbf{q}(x)$, $x = 1, \dots, N$, its corresponding asymmetric self-attention is

$$\mathbf{u}(x) = \sum_{y=1}^N \text{softmax} \left(\frac{\mathbf{q}(x)^\top \mathbf{k}(y)}{\sqrt{D_{qk}}} \right) \|\mathbf{v}(x) - \mathbf{v}(y)\|^{p-2} \mathbf{v}(y) \quad (11)$$

With (11), we are now ready to define the p -Laplacian Transformers (p -LaT).

Definition 3.1 (p -Laplacian Transformers). *For each layer $l = 1, \dots, L$ of p -LaT, the set of query, key and value vectors $\{\mathbf{q}^l(x), \mathbf{k}^l(x), \mathbf{v}^l(x)\}_{x=1}^N$ of output sequence $\mathbf{U}^{l-1} := [\mathbf{u}^{l-1}(1), \dots, \mathbf{u}^{l-1}(N)]^\top \in \mathbb{R}^{N \times D}$ in the previous layer will be set by formulae in (1). And the corresponding output vector $\mathbf{u}^l(x)$, $x = 1, \dots, N$ of layer l -th will be computed by the following attention formula with arbitrary p value*

$$\mathbf{u}^l(x) = \sum_{y=1}^N \text{softmax} \left(\frac{\mathbf{q}^l(x)^\top \mathbf{k}^l(y)}{\sqrt{D_{qk}}} \right) \mathbf{p}^l(x, y) \mathbf{v}^l(y) \\ \mathbf{p}^l(x, y) = \|\mathbf{v}^l(x) - \mathbf{v}^l(y)\|^{p-2} \quad (12)$$

Remark 3.2. \mathbf{U}^0 sequence is identical to the input sequence $\mathbf{X} := [\mathbf{x}(1), \dots, \mathbf{x}(N)]^\top \in \mathbb{R}^{N \times D_x}$ of the Transformers.

Remark 3.3. Rewrite (12) in a matrix form we obtain $\mathbf{U}_l = \text{softmax}(\mathbf{Q}_l \mathbf{K}_l^\top / \sqrt{D_{qk}}) \mathbf{P}_l \mathbf{V}_l$ where $\mathbf{P}_l \in \mathbb{R}^{N \times N}$ and the position (x, y) in that matrix has the value of $\mathbf{P}_l(x, y) = \|\mathbf{v}^l(x) - \mathbf{v}^l(y)\|^{p-2}$.

We present the following theorem to show the convergence property of p -LaT.

Theorem 3.4. *Given sequence $\mathbf{U}^l := [\mathbf{u}^l(1), \dots, \mathbf{u}^l(N)]^\top \in \mathbb{R}^{N \times D}$ is the output of p -LaT at layer l -th and the J defined in (3). Then*

$$J(\mathbf{U}^l) \geq J(\mathbf{U}^{l+1}) \quad (13)$$

Theorem 3.4 shows that the functional in (3), or the objective function, is guaranteed to decline after taking one layer of p -LaT.

Proof. To prove the theorem, we need to show that the right-hand side of (7) is the direction of steepest descent and minimizes $J(\mathbf{u})$.

Again, for notational simplicity, we define $L(x) = \int_{\Omega} K(x, y) \|\mathbf{u}(x) - \mathbf{u}(y)\|^{p-2} (\mathbf{u}(x) - \mathbf{u}(y)) dy$. From the left-hand-side of (5), we recall that

$$\left. \frac{d}{dt} \right|_{t=0} J(\mathbf{u} + t\mathbf{h}) = \int_{\Omega^2} K(x, y) \|\mathbf{u}(x) - \mathbf{u}(y)\|^{p-2} (\mathbf{u}(x) - \mathbf{u}(y)) \mathbf{h}(x) dx dy \\ = \left\langle \int_{\Omega} K(x, y) \|\mathbf{u}(x) - \mathbf{u}(y)\|^{p-2} (\mathbf{u}(x) - \mathbf{u}(y)) dy, \mathbf{h}(x) \right\rangle_{L^2(\Omega)} \\ = \langle L(x), \mathbf{h}(x) \rangle_{L^2(\Omega)}$$

Then using the Cauchy-Schwarz inequality,

$$\left| \left. \frac{d}{dt} \right|_{t=0} J(\mathbf{u} + t\mathbf{h}) \right| \leq \|L(x)\| \cdot \|\mathbf{h}(x)\|$$

the equality happens iff $\mathbf{h}(x) = \alpha L(x)$ with a positive number α . This implies that the direction $\mathbf{h}(x) = \alpha L(x)$ is the direction of the steepest ascent and maximizes $J(\mathbf{u})$. And thus $-L(x) = -\int_{\Omega} K(x, y) \|\mathbf{u}(x) - \mathbf{u}(y)\|^{p-2} (\mathbf{u}(x) - \mathbf{u}(y)) dy$ points in the direction of steepest descent, and the flow in (7) tends to move toward a state of lesser energy. \square

4 Spectral Analysis of p -LaT

In this section, we embark on a spectral analysis journey to unveil the distinct characteristics of p -LaT that set them apart from traditional Transformers. Specifically, we focus on demonstrating that (11) does not conform to the attributes of a conventional low-pass filter.

Our analytical tool of choice is the Fourier transform, which serves as a powerful instrument in our investigation. To lay the foundation for our spectral analysis, we begin by revisiting the fundamentals of Fourier analysis and the definition of endomorphism low-pass filters, as outlined in Wang et al. (2022).

Denote $\mathcal{F} : \mathbb{R}^n \rightarrow \mathbb{C}^n$ be the Discrete Fourier Transform (DFT) with the Inverse Discrete Fourier Transform (IDFT) $\mathcal{F}^{-1} : \mathbb{C}^n \rightarrow \mathbb{R}^n$. $\mathbf{f}_k = [e^{2\pi j(k-1) \cdot 0} \dots e^{2\pi j(k-1) \cdot (n-1)}]^\top / \sqrt{n} \in \mathbb{R}^n$ where k denotes the k -th row of DFT matrix, and j is the imaginary unit.

Let $\tilde{z} = \mathcal{F}z$ be the spectrum of z , and $\tilde{z}_{dc} \in \mathbb{C}$, $\tilde{z}_{hc} \in \mathbb{C}^{n-1}$ take the first element and the rest elements of \tilde{z} , respectively. Define $\mathcal{DC}[z] = \tilde{z}_{dc} \mathbf{f}_1 \in \mathbb{C}^n$ as the Direct-Current (DC) component of signal z , and $\mathcal{HC}[z] = [\mathbf{f}_2 \dots \mathbf{f}_n] \tilde{z}_{hc} \in \mathbb{C}^n$ the complementary high-frequency component. A low-pass filter is a system that suppresses the high-frequency component of signals and retains the low-frequency component. Thus,

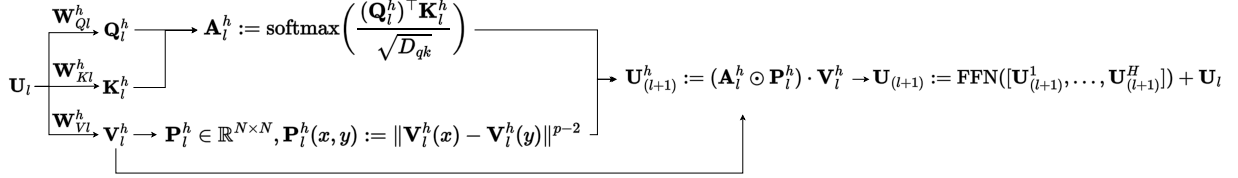


Figure 1: Architecture of a p -Laplacian Transformer at one head. We denote H is the number of heads and $h = 1, \dots, H$. The set query, key, value matrices at layer l -th and head h -th are denoted as $\{\mathbf{Q}_l^h; \mathbf{K}_l^h; \mathbf{V}_l^h\}$. Also, FFN is the feed-forward layer and $[\mathbf{U}_{(l+1)}^1; \dots; \mathbf{U}_{(l+1)}^H]$ is the concatenate operator.

a low-pass filter will only preserve the DC component, while diminishing the remaining HC component.

Definition 4.1. Given an endomorphism $f : \mathbb{R}^N \rightarrow \mathbb{R}^N$, f is a low-pass filter if and only if

$$\lim_{t \rightarrow \infty} \frac{\|\mathcal{H}\mathcal{C}(f^t z)\|}{\|\mathcal{D}\mathcal{C}(f^t z)\|} = 0, \quad \forall z \in \mathbb{R}^N.$$

The main result of that paper is that self-attention is constantly a low-pass filter. More precisely, they proved the following theorem.

Theorem 4.2 (Wang et al. (2022)). Let $\mathbf{A} = \text{softmax}(\mathbf{P})$, where $\mathbf{P} \in \mathbb{R}^{n \times n}$. Then \mathbf{A} must be a low-pass filter for all $z \in \mathbb{R}^n$:

$$\lim_{t \rightarrow \infty} \frac{\|\mathcal{H}\mathcal{C}[\mathbf{A}^t z]\|}{\|\mathcal{D}\mathcal{C}[\mathbf{A}^t z]\|} = 0 \quad (14)$$

Since \mathbf{A} is the output of softmax function, i.e. a right-stochastic matrix, it has the largest eigenvalue $\lambda_{max} = 1$. We found that the need for \mathbf{A} to be a right-stochastic matrix is a tight condition. In fact, we can loosen up and make the theorem more general. We state the following theorem

Theorem 4.3. Let \mathbf{A} be a positive matrix, in which it has $\lambda_{max} \leq 1$. Then \mathbf{A} must be a low-pass filter for all $z \in \mathbb{R}^n$:

$$\lim_{t \rightarrow \infty} \frac{\|\mathcal{H}\mathcal{C}[\mathbf{A}^t z]\|}{\|\mathcal{D}\mathcal{C}[\mathbf{A}^t z]\|} = 0 \quad (15)$$

To prove the theorem, we only need to make a slight modification in the proof of the original paper.

Moreover, we can establish the subsequent theorem, which represents the converse of Theorem 4.3. It effectively demonstrates how, through the application of p -Laplacian regularization, we can mitigate the effects of low-pass filters. While Theorem 4.3 may not stand as a central theorem in our research, it forms an indispensable stepping stone, laying the groundwork for the theorem that follows.

Theorem 4.4. Let \mathbf{A} be a low-pass filter. If $\mathbf{1}$ is not the eigenvector correspond to λ_{max} , then we have $\lambda_{max} \leq 1$.

Proof. We now prove the Theorem 4.4 by contradiction. We assume that $\mathbf{1}$ is not an eigenvector associated with λ_{max} , $\lambda_{max} > 1$, and

$$\lim_{t \rightarrow \infty} \frac{\|\mathcal{H}\mathcal{C}(A^t z)\|}{\|\mathcal{D}\mathcal{C}(A^t z)\|} = 0, \text{ for all } z \in \mathbb{R}^N.$$

We will try to deduce a contradiction.

The Perron-Frobenius theorem (Meyer and Stewart, 2023) claims that there is a positive vector (element-wise) y such that $\mathbf{A}y = \lambda_{max}y$. This implies $\mathbf{A}^t y = \lambda_{max}^t y$. Insert this equality into the above term, we get

$$\begin{aligned} \lim_{t \rightarrow \infty} \frac{\|\mathcal{H}\mathcal{C}(\mathbf{A}^t y)\|}{\|\mathcal{D}\mathcal{C}(\mathbf{A}^t y)\|} &= \lim_{t \rightarrow \infty} \sqrt{\frac{\|\mathcal{H}\mathcal{C}(\mathbf{A}^t y)\|^2}{\|\mathcal{D}\mathcal{C}(\mathbf{A}^t y)\|^2}} \\ &= \lim_{t \rightarrow \infty} \sqrt{\frac{\|\lambda_{max}^t (I - \frac{1}{N} \mathbf{1}\mathbf{1}^T)y\|^2}{\|y - \lambda_{max}^t (I - \frac{1}{N} \mathbf{1}\mathbf{1}^T)y\|^2}} \end{aligned} \quad (16)$$

Since we assume that the vector y is not a multiplication of $\mathbf{1}$, the last term in 16 is equal to 1. \square

The significance of Theorem 4.4 lies in its capacity to elucidate how achieving $\lambda_{max} > 1$ can disrupt the low-pass filter characteristics inherent in \mathbf{A} . We can attain this condition, for example, when $\sum_j \mathbf{A}_{ij} \geq 1, \forall i$ and there exists at least one row that $\sum_j \mathbf{A}_{ij} > 1$.

Given the unavailability of token labels within the intermediate layers of Transformers, we define homophily and heterophily in terms of features vectors similarity and dissimilarity.

Definition 4.5. For a specific layer, denoted as the l -th layer of the Transformers, we characterize the implicit structure as homophily when it satisfies:

$$\|\mathbf{v}^l(x) - \mathbf{v}^l(y)\| < 1, \quad \forall x, y$$

In contrast, the implicit structure is classified as heterophily if it meets the condition:

$$\|\mathbf{v}^l(x) - \mathbf{v}^l(y)\| \geq 1, \quad \forall x, y$$

Table 1: Top-1 and Top-5 accuracy (%) of p -LaT vs DeiT on the ImageNet benchmark.

Model	Top-1 Acc (%)	Top-5 Acc (%)
DeiT	71.97	91.13
p -LaT	72.78	91.31

Table 2: Test and valid perplexity (Test PPL and Valid PPL) on WikiText-103 of p -LaT compared to the conventional softmax transformer.

Model	Valid PPL	Test PPL
Softmax Transformer	33.17	34.1
p -LaT	32.57	33.5

The introduction of the p -laplacian term, $\|\mathbf{v}(x) - \mathbf{v}(y)\|^{p-2}$, leads to a transformation in the eigenvalue characteristics. Specifically, the presence of the p -laplacian term results in $\lambda_{max} > 1$ for the p -LaT, rendering matrix \mathbf{A} as a non-low-pass filter.

For the case of $p < 2$, the p -LaT model escapes from low-pass filters situation for $\|\mathbf{v}(x) - \mathbf{v}(y)\| < 1, \forall x, y$. This observation highlights the effectiveness of the p -LaT model in the case of strong homophily structure.

Conversely, for the scenario where $p > 2$, the p -LaT model no longer acts as a low-pass filter for $\|\mathbf{v}(x) - \mathbf{v}(y)\| > 1, \forall x, y$. This underscores the p -LaT model’s proficiency in modeling strong heterophily structure.

Remark 4.6. *In the form of matrix, \mathbf{A} in the case of p -LaT is defined as $\mathbf{A} := \text{softmax}(\mathbf{Q}^\top \mathbf{K} / \sqrt{D_{qk}}) \mathbf{P}$. Where $\mathbf{P} \in \mathbb{R}^{N \times N}$ and the position (x, y) in that matrix has the value of $\mathbf{P}(x, y) := \|\mathbf{V}(x) - \mathbf{V}(y)\|^{p-2}$.*

5 Experimental Results

In this section, we empirically demonstrate the advantages of our proposed p -LaT approach across various tasks, including ImageNet classification (Deng et al., 2009) and language modeling on the WikiText-103 (Merity et al., 2016). All experiments were conducted on a single DGX-A100 system.

Object classification on ImageNet. To demonstrate the advantage of our method, we compare it with the DeiT baseline (Touvron et al., 2021) on the ImageNet image classification task. The ImageNet dataset (Deng et al., 2009) comprises 1.28 million training images and 50,000 validation images, encompassing the classification of 1000 categories. The evaluation metrics used for performance assessment are the top-1 and top-5 accuracies.

Models settings for Imagenet. Our baseline model is the DeiT-tiny model (Touvron et al., 2021), which consists of 12 transformer layers, 3 attention heads per layer, and a model dimension of 192. For model setting

and setting and configuration, we follow Touvron et al. (2021). For p -LaT, we follow the same parameters settings, the difference is that we set 2 attention heads with low p value ($p = 1.5$), and the other 2 heads with high p value ($p = 2.5$). Figure 1 represents our architecture.

Our p -LaT outperforms the DeiT baseline, demonstrating superior performance in both Top-1 Accuracy and Top-5 Accuracy metrics, as illustrated in Table 1.

Language Model on WikiText-103. In addition to computer vision tasks, we also evaluate the effectiveness of our model on a large-scale natural language processing application, specifically language modeling on WikiText-103. The WikiText-103 dataset is a carefully curated collection of articles sourced from Wikipedia, designed to capture intricate and extensive contextual dependencies. The training set comprises a substantial 28,000 articles, totaling an impressive 103 million running words. Each article is structured into text blocks, each spanning around 3,600 words. Moving to the validation and test sets, they encompass 218,000 and 246,000 running words, respectively, each composed of 60 articles totaling approximately 268,000 words. Our experimental framework adheres to standard practices (Schlag et al., 2021; Merity et al., 2016), which involve segmenting the training data into independent sequences, each comprising L words. For our evaluation, we employ a batch size of 1 and process the text sequence through a sliding window of size L . When assessing perplexity (PPL), we exclusively consider the final position, except for the initial segment where all positions are comprehensively evaluated, in alignment with the approach outlined in Schlag et al. (2021); Al-Rfou et al. (2019). For our language modeling implementation, we rely on the publicly available code developed by Schlag et al. (2021).

Model settings for WikiText-103. In our experiments, we set the dimensions of keys, values, and queries to 128, while the training and evaluation context length is set to 256. Again, for p -LaT, we follow the same parameters settings, the difference is that we

set 4 attention heads with low p value ($p = 1.5$), and the other 4 heads with high p value ($p = 2.5$).

As indicated in Table 2, our p -LaT language model showcases superior performance, excelling in both test and valid perplexity metrics when contrasted with the softmax transformer language model (Xiong et al., 2021). These empirical outcomes, complemented by the success observed in diverse tasks, provide robust evidence of the substantial advantages offered by our p -LaT models.

6 Related Work

Transformers. Transformers have left an indelible mark on various domains, with foundational work introducing the Transformer model (Vaswani et al., 2017), and variations like BERT (Devlin et al., 2018) and GPT (Brown et al., 2020) extending its applications in NLP. They’ve revolutionized transfer learning, with models like RoBERTa (Liu et al., 2019) leading the way, while Vision Transformers (ViTs) (Dosovitskiy et al., 2020) bring the Transformer architecture to computer vision. Efficiency-focused models like DistilBERT (Sanh et al., 2019) and MobileBERT (Sun et al., 2020) maintain performance while reducing model size. In summary, Transformers continue to shape NLP, computer vision, and other domains, owing to their adaptability, transfer learning capacity, and versatility. However, it still has limitation. Dong et al. (2021); Wang et al. (2022) investigate Transformers in the image domain through the lens of Fourier spectrum, showing that self-attentions are low-pass filters, retaining only low-frequency, causing over-smoothed outputs. Our work is an orthogonal explanation of the previous work, providing a variational perspective of the low-frequency phenomenon and deriving the novel p -LaT method to obtain non-low frequencies and improve the performances under implicit homophilic/heterophilic structures.

p -Laplacian Regularization Framework. The application of p -Laplacian regularization in image processing, particularly in the domain of denoising, has gained substantial attention. p -Laplacian regularization is a powerful tool for reducing noise while preserving essential image features. Prior studies such as Pang and Cheung (2017) and Elmoataz et al. (2015) have explored the use of p -Laplacian regularization to enhance image denoising techniques. These works emphasize the effectiveness of p -Laplacian regularization in improving the quality of denoised images, making it a prominent approach in the field. Additionally, in the realm of machine learning, Fu et al. (2022) harnesses p -Laplacian regularization to address heterophily challenges within discrete graphs. Notably,

Calder (2018) and Slepcev and Thorpe (2019) conduct thorough analyses of p -Laplacian regularization, particularly in semi-supervised and regression tasks, showcasing its competence when working with limited training data. It’s noteworthy that the original p -Laplacian regularization is defined as follows:

$$J(\mathbf{u}) = \frac{1}{p} \int_{\Omega^2} k(x, y) \|\mathbf{u}(y) - \mathbf{u}(x)\|^p dy dx + \mu \|\mathbf{u} - \mathbf{x}\|^2$$

Here, the first term quantifies signal variation over image patches or networks, while the second term enforces constraints to prevent excessive deviation from the input signal \mathbf{x} . The parameter $\mu \in (0, \infty)$ governs the balance between these constraints. In our work, we set $\mu = 0$ to explore how traditional Transformers evolve with varying values of p .

7 Conclusion

In this study, we leveraged the p -Laplacian regularization framework to illuminate the inner workings of Transformers’ representations. This exploration deepened our understanding and introduced pathways for performance enhancement. Under spectral analysis, our work unveiled p -Laplacian regularization as a versatile framework for self-attention mechanisms, guarantees in convergence and harnessing the concepts of both homophily and heterophily within Transformers to amplify their capabilities. We validated our approach through empirical assessments across large-scale applications, encompassing ImageNet object classification and WikiText-103 language modeling. However, it’s important to acknowledge that our study does not address the robustness of our model to perturbed data. This presents an intriguing avenue for future research—exploring how the comprehensive p -Laplacian framework can bolster the robustness of Transformer models. We leave this idea for future investigation.

References

Tom Brown, Benjamin Mann, Nick Ryder, Melanie Subbiah, Jared D Kaplan, Prafulla Dhariwal, Arvind Neelakantan, Pranav Shyam, Girish Sastry, Amanda Askell, et al. Language models are few-shot learners. *Advances in neural information processing systems*, 33:1877–1901, 2020.

Zihang Dai, Zhilin Yang, Yiming Yang, Jaime Carbonell, Quoc V Le, and Ruslan Salakhutdinov. Transformer-xl: Attentive language models beyond a fixed-length context. *arXiv preprint arXiv:1901.02860*, 2019.

Colin Raffel, Noam Shazeer, Adam Roberts, Katherine Lee, Sharan Narang, Michael Matena, Yanqi Zhou,

- Wei Li, and Peter J Liu. Exploring the limits of transfer learning with a unified text-to-text transformer. *The Journal of Machine Learning Research*, 21(1):5485–5551, 2020.
- Lili Chen, Kevin Lu, Aravind Rajeswaran, Kimin Lee, Aditya Grover, Misha Laskin, Pieter Abbeel, Aravind Srinivas, and Igor Mordatch. Decision transformer: Reinforcement learning via sequence modeling. *Advances in neural information processing systems*, 34:15084–15097, 2021.
- Alexey Dosovitskiy, Lucas Beyer, Alexander Kolesnikov, Dirk Weissenborn, Xiaohua Zhai, Thomas Unterthiner, Mostafa Dehghani, Matthias Minderer, Georg Heigold, Sylvain Gelly, et al. An image is worth 16x16 words: Transformers for image recognition at scale. *arXiv preprint arXiv:2010.11929*, 2020.
- Ze Liu, Yutong Lin, Yue Cao, Han Hu, Yixuan Wei, Zheng Zhang, Stephen Lin, and Baining Guo. Swin transformer: Hierarchical vision transformer using shifted windows. In *Proceedings of the IEEE/CVF international conference on computer vision*, pages 10012–10022, 2021.
- Anurag Arnab, Mostafa Dehghani, Georg Heigold, Chen Sun, Mario Lučić, and Cordelia Schmid. Vivit: A video vision transformer. In *Proceedings of the IEEE/CVF international conference on computer vision*, pages 6836–6846, 2021.
- Meng-Hao Guo, Jun-Xiong Cai, Zheng-Ning Liu, Tai-Jiang Mu, Ralph R Martin, and Shi-Min Hu. Pct: Point cloud transformer. *Computational Visual Media*, 7:187–199, 2021.
- Alexander Rives, Joshua Meier, Tom Sercu, Siddharth Goyal, Zeming Lin, Jason Liu, Demi Guo, Myle Ott, C Lawrence Zitnick, Jerry Ma, et al. Biological structure and function emerge from scaling unsupervised learning to 250 million protein sequences. *Proceedings of the National Academy of Sciences*, 118(15):e2016239118, 2021.
- John Jumper, Richard Evans, Alexander Pritzel, Tim Green, Michael Figurnov, Olaf Ronneberger, Kathryn Tunyasuvunakool, Russ Bates, Augustin Žídek, Anna Potapenko, et al. Highly accurate protein structure prediction with alphafold. *Nature*, 596(7873):583–589, 2021.
- Anmol Gulati, James Qin, Chung-Cheng Chiu, Niki Parmar, Yu Zhang, Jiahui Yu, Wei Han, Shibo Wang, Zhengdong Zhang, Yonghui Wu, et al. Conformer: Convolution-augmented transformer for speech recognition. *arXiv preprint arXiv:2005.08100*, 2020.
- Shuai Zhang, Lina Yao, Aixin Sun, and Yi Tay. Deep learning based recommender system: A survey and new perspectives. *ACM computing surveys (CSUR)*, 52(1):1–38, 2019.
- Alec Radford, Karthik Narasimhan, Tim Salimans, Ilya Sutskever, et al. Improving language understanding by generative pre-training. 2018.
- Alec Radford, Jeffrey Wu, Rewon Child, David Luan, Dario Amodei, Ilya Sutskever, et al. Language models are unsupervised multitask learners. *OpenAI blog*, 1(8):9, 2019.
- Jacob Devlin, Ming-Wei Chang, Kenton Lee, and Kristina Toutanova. Bert: Pre-training of deep bidirectional transformers for language understanding. *arXiv preprint arXiv:1810.04805*, 2018.
- Yinhan Liu, Myle Ott, Naman Goyal, Jingfei Du, Mandar Joshi, Danqi Chen, Omer Levy, Mike Lewis, Luke Zettlemoyer, and Veselin Stoyanov. Roberta: A robustly optimized bert pretraining approach. *arXiv preprint arXiv:1907.11692*, 2019.
- Ashish Vaswani, Noam Shazeer, Niki Parmar, Jakob Uszkoreit, Llion Jones, Aidan N Gomez, Łukasz Kaiser, and Illia Polosukhin. Attention is all you need. *Advances in neural information processing systems*, 30, 2017.
- Jesse Vig and Yonatan Belinkov. Analyzing the structure of attention in a transformer language model. *arXiv preprint arXiv:1906.04284*, 2019.
- Elena Voita, David Talbot, Fedor Moiseev, Rico Senrich, and Ivan Titov. Analyzing multi-head self-attention: Specialized heads do the heavy lifting, the rest can be pruned. *arXiv preprint arXiv:1905.09418*, 2019.
- Yongchun Gu, Yi Wang, Heng-Ru Zhang, Jiao Wu, and Xingquan Gu. Enhancing text classification by graph neural networks with multi-granular topic-aware graph. *IEEE Access*, 11:20169–20183, 2023.
- Xiang Li, Renyu Zhu, Yao Cheng, Caihua Shan, Siqiang Luo, Dongsheng Li, and Weining Qian. Finding global homophily in graph neural networks when meeting heterophily. In *International Conference on Machine Learning*, pages 13242–13256. PMLR, 2022.
- Peihao Wang, Wenqing Zheng, Tianlong Chen, and Zhangyang Wang. Anti-oversmoothing in deep vision transformers via the fourier domain analysis: From theory to practice. *arXiv preprint arXiv:2203.05962*, 2022.
- Guy Gilboa and Stanley Osher. Nonlocal operators with applications to image processing. *Multiscale Modeling & Simulation*, 7(3):1005–1028, 2009.
- Leonid I Rudin, Stanley Osher, and Emad Fatemi. Nonlinear total variation based noise removal algo-

- rithms. *Physica D: nonlinear phenomena*, 60(1-4): 259–268, 1992.
- Xiaolong Wang, Ross Girshick, Abhinav Gupta, and Kaiming He. Non-local neural networks. In *Proceedings of the IEEE conference on computer vision and pattern recognition*, pages 7794–7803, 2018.
- Prajit Ramachandran, Niki Parmar, Ashish Vaswani, Irwan Bello, Anselm Levskaya, and Jon Shlens. Stand-alone self-attention in vision models. *Advances in neural information processing systems*, 32, 2019.
- Carl D Meyer and Ian Stewart. *Matrix analysis and applied linear algebra*. SIAM, 2023.
- Jia Deng, Wei Dong, Richard Socher, Li-Jia Li, Kai Li, and Li Fei-Fei. Imagenet: A large-scale hierarchical image database. In *2009 IEEE conference on computer vision and pattern recognition*, pages 248–255. Ieee, 2009.
- Stephen Merity, Caiming Xiong, James Bradbury, and Richard Socher. Pointer sentinel mixture models. *arXiv preprint arXiv:1609.07843*, 2016.
- Hugo Touvron, Matthieu Cord, Matthijs Douze, Francisco Massa, Alexandre Sablayrolles, and Hervé Jégou. Training data-efficient image transformers & distillation through attention. In *International conference on machine learning*, pages 10347–10357. PMLR, 2021.
- Imanol Schlag, Kazuki Irie, and Jürgen Schmidhuber. Linear transformers are secretly fast weight programmers. In *International Conference on Machine Learning*, pages 9355–9366. PMLR, 2021.
- Rami Al-Rfou, Dokook Choe, Noah Constant, Mandy Guo, and Llion Jones. Character-level language modeling with deeper self-attention. In *Proceedings of the AAAI conference on artificial intelligence*, volume 33, pages 3159–3166, 2019.
- Yunyang Xiong, Zhanpeng Zeng, Rudrasis Chakraborty, Mingxing Tan, Glenn Fung, Yin Li, and Vikas Singh. Nyströmformer: A nyström-based algorithm for approximating self-attention. In *Proceedings of the AAAI Conference on Artificial Intelligence*, volume 35, pages 14138–14148, 2021.
- Victor Sanh, Lysandre Debut, Julien Chaumond, and Thomas Wolf. Distilbert, a distilled version of bert: smaller, faster, cheaper and lighter. *arXiv preprint arXiv:1910.01108*, 2019.
- Zhiqing Sun, Hongkun Yu, Xiaodan Song, Renjie Liu, Yiming Yang, and Denny Zhou. Mobilebert: a compact task-agnostic bert for resource-limited devices. *arXiv preprint arXiv:2004.02984*, 2020.
- Yihe Dong, Jean-Baptiste Cordonnier, and Andreas Loukas. Attention is not all you need: Pure attention loses rank doubly exponentially with depth. In *International Conference on Machine Learning*, pages 2793–2803. PMLR, 2021.
- Jiahao Pang and Gene Cheung. Graph laplacian regularization for image denoising: Analysis in the continuous domain. *IEEE Transactions on Image Processing*, 26(4):1770–1785, 2017.
- Abderrahim Elmoataz, Matthieu Toutain, and Daniel Tenbrinck. On the *p*-laplacian and ∞ -laplacian on graphs with applications in image and data processing. *SIAM Journal on Imaging Sciences*, 8(4):2412–2451, 2015.
- Guoji Fu, Peilin Zhao, and Yatao Bian. *p*-laplacian based graph neural networks. In *International Conference on Machine Learning*, pages 6878–6917. PMLR, 2022.
- Jeff Calder. The game theoretic *p*-laplacian and semi-supervised learning with few labels. *Nonlinearity*, 32(1):301, 2018.
- Dejan Slepcev and Matthew Thorpe. Analysis of *p*-laplacian regularization in semisupervised learning. *SIAM Journal on Mathematical Analysis*, 51(3):2085–2120, 2019.